

Raman and infrared spectra of the $(\text{CuInSe}_2)_{1-x}-(2\text{ZnSe})_x$ system*

J. N. Gan and J. Tauc[†]

Department of Physics and Division of Engineering, Brown University, Providence, Rhode Island 02912

V. G. Lambrecht, Jr. and M. Robbins

Bell Laboratories, Murray Hill, New Jersey 07974

(Received 22 September 1975)

The effects of crystal symmetry and disorder on the infrared and Raman spectra of the solid solution $(\text{CuInSe}_2)_{1-x}-(2\text{ZnSe})_x$ were studied. This system crystallizes in the chalcopyrite structure for $x \leq 0.43$ and in the zinc-blende structure for $x \geq 0.48$. Significant differences were found for the spectra of the mixtures and the spectra of the end compounds. Large shifts and broadening in the infrared reststrahlen and Raman bands indicate the excitations of vibrational modes with $\vec{k} \neq 0$ induced by substitutional disorder. As a result, the spectra of the mixtures reveal the density of vibrational states throughout the Brillouin zone. The symmetries of the observed modes were assigned from the polarization and composition dependences.

INTRODUCTION

We measured the Raman and infrared spectra on single crystals of the solid solution of a ternary compound CuInSe_2 with a binary compound ZnSe which is its electronic analog. The system $(\text{CuInSe}_2)_{1-x}-(2\text{ZnSe})_x$ crystallizes in the chalcopyrite (ch) structure for $x \leq 0.43$ and in the zinc-blende (zb) structure for $x \geq 0.48$.¹ Both structures are based on tetrahedral bonding and are closely related.² Since the ratio c/a , in the ch structure, is equal to two (within 1%) in the whole composition range, the unit cell of the ch structure is almost exactly equal to two unit cells of the zb structure. The system is suitable for studying the effects of the change in the crystal symmetry and of the disorder. In the solid solutions, there is a periodic lattice but the basis atoms are not identical in each cell. In the mixtures with the ch structure, Cu and In are ordered relative to each other but are randomly replaced by the Zn atoms. In the zb structure, Cu, In, and Zn atoms are randomly distributed around the Se atoms.

The vibrational spectra of ZnSe have been studied by Irwin and LaCombe.³ Several authors did work on other $\text{A}^{\text{I}}\text{B}^{\text{III}}\text{C}_2^{\text{VI}}$ compounds with the chalcopyrite structure, in particular, CuGaS_2 ,^{4,5} AgGaS_2 ,⁵⁻⁸ AgGaSe_2 ,^{5,7} and CuAlS_2 ,⁹ but there are no previous studies of lattice vibrations in CuInSe_2 . From the measured polarized Raman and ir spectra we found the symmetry assignments of the modes in this ternary compound.

We studied single crystals of the solid solutions with $x = 0.08, 0.21, 0.29, 0.33, 0.43, 0.48,$ and 0.6 prepared by directional freezing in horizontal boats or by the Bridgman method as described previously.¹ Samples of good crystallinity were selected and oriented using the back-reflection Laue method, and then polished with Linde 0.3- μm alumina abrasive and finally with Syton. On these

samples, we could follow the changes in the spectra as the composition is varied from $x = 0$ to $x = 1$.

EXPERIMENTAL TECHNIQUES

The infrared reflectivity was measured with a Digilab Fourier Transform Spectrometer Model FTS-14 from 50 to 500 cm^{-1} . In our experiments, the number of scans for each sample was 1000. A NOVA 1200 minicomputer was used to process the results.

For Raman scattering, we used the 5145- \AA line of a coherent radiation model 52 argon laser. The scattered light was analyzed by a Jarrell-Ash Czerney-Turner double-grating monochromator. The output was detected by an ITT FW-130 cooled photon counter was used to count the photons and 1120 amplifier-discriminator. An SSR Model 1110 phonon counter was used to count the photons and the results were punched out on paper tape by a teletype. Simultaneously, an Elscint ratemeter was used to obtain a continuous plot. To increase the signal-to-noise ratio for very weak signals, we used a signal averager to store repetitive scans.

SYMMETRY OF THE VIBRATIONAL MODES

The point group of the zb structure is T_d^2 while the chalcopyrite structure belongs to D_{2d} . The character tables of important symmetry points are published in Ref. 10 and 11. Both structures are closely related, and we can study how a vibrational mode in the zb structure transforms if the structure changes to chalcopyrite. Consider a state G_i in the zb Brillouin zone. If we find that the direct product $G_i \times G'_j$ (where G'_j represents a state in the ch Brillouin zone) contains G'_j , then G'_j is compatible with G_i . Similarly, one may find that $G_i \times G'_k$ also contains G'_k . Then, the state G_i in the zinc-blende structure is said to split up into G'_j and G'_k in the chalcopyrite structure. In

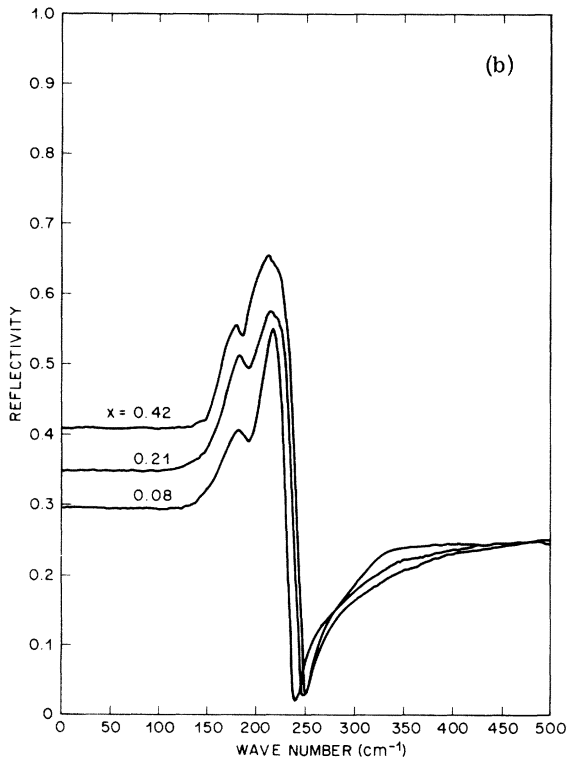
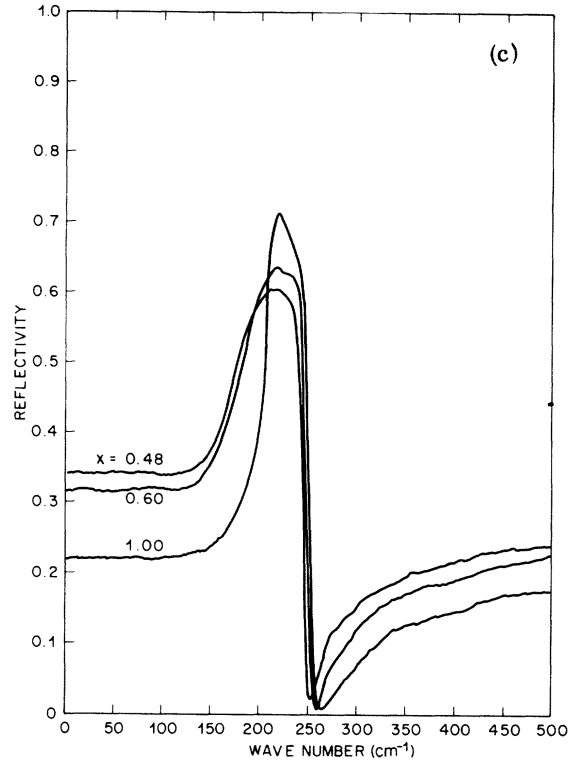
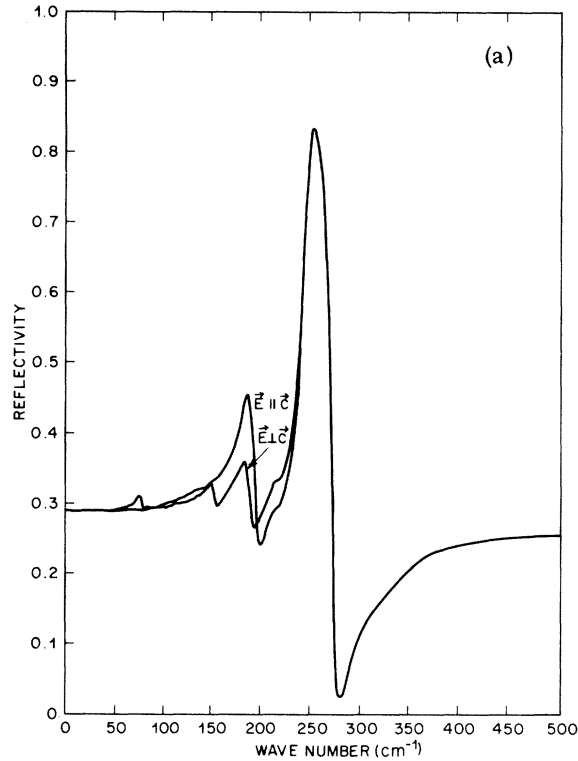


FIG. 1. (a) Polarized infrared reflectivity of CuInSe_2 . (b) Unpolarized infrared reflectivity for mixed compounds with the chalcopyrite structure. (c) Unpolarized infrared reflectivity for mixed compounds with the zinc-blende structure and for ZnSe .

tables.¹³

The chalcopyrite unit cell contains eight atoms giving rise to 24 modes of vibrations. Of these 24 modes, 21 are optic modes and three are acoustic modes. The optic phonons transform like $\Gamma_1 + 2\Gamma_2 + 3\Gamma_3 + 3\Gamma_4 + 12\Gamma_5$ and the acoustic phonons transform like $\Gamma_4 + 2\Gamma_5$.^{14,15} All optic modes except two Γ_2 modes are Raman active. Only the Γ_4 and Γ_5 modes are infrared active.

INFRARED SPECTRA

The infrared reflectivity measurements for various compositions of the system are shown in Figs. 1(a)–1(c). Four reststrahlen bands were observed for the pure CuInSe_2 crystal, two for the mixed compounds with the chalcopyrite structure and one for the mixed compounds with the zinc-blende structure. From the reflection spectra, we calculated ϵ_2 and $\text{Im}(-1/\epsilon)$ by Kramers-Kronig analysis. The TO and LO modes are identified from the maxima of ϵ_2 and $\text{Im}(-1/\epsilon)$, respectively. E modes are allowed only for $\vec{E} \perp \vec{c}$ while B modes are allowed only for $\vec{E} \parallel \vec{c}$. The TO and LO modes observed for various compositions of the $(\text{CuInSe}_2)_{1-x}-(2\text{ZnSe})_x$ system are given in Table II.

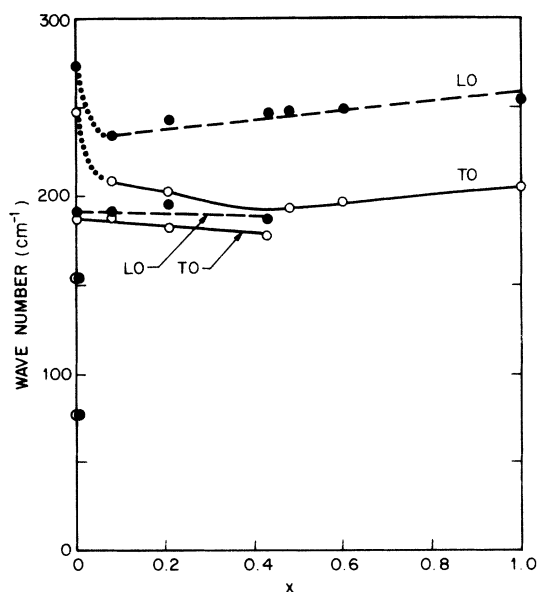
Table I, we give the symmetry mapping from vibrational states in the zinc-blende to the zone-center modes in the chalcopyrite structure obtained by the above considerations¹² or from published

TABLE I. Symmetry mapping for the vibrational states of zinc-blende and chalcopyrite structures.

Zinc blende	Chalcopyrite
$\Gamma_{15}(\text{LO})$	$\Gamma_4 + \Gamma_5$
X_1	Γ_2
W_2	$\Gamma_3 + \Gamma_4$
W_4	Γ_5
$\Gamma_{15}(\text{TO})$	$\Gamma_4 + \Gamma_5$
X_5	Γ_5
W_1	Γ_1
X_3	Γ_3
W_3	Γ_5

In Fig. 2, we plot the frequencies of the infrared modes as a function of composition. The two modes with the highest frequencies (at 274 and 248 cm^{-1} in CuInSe_2) were observed throughout the whole range of compositions for both polarizations $\vec{E} \perp \vec{c}$ and $\vec{E} \parallel \vec{c}$. Their presence in the zinc-blende phase indicates that these modes must be the $\Gamma_{15}(\text{LO})$ and $\Gamma_{15}(\text{TO})$ modes in the zinc-blende structure. When the structure becomes chalcopyrite, these modes become the $\Gamma_4 + \Gamma_5$ TO and LO modes. Since these modes contain both Γ_4 and Γ_5 symmetries, they can be observed in infrared reflectivity for both $\vec{E} \perp \vec{c}$ and $\vec{E} \parallel \vec{c}$.

The most interesting feature of the composition dependence of these reststrahlen bands is the sudden dip of the frequency when x changes from 0 to 0.08.

FIG. 2. Infrared-active modes vs composition for the $(\text{CuInSe}_2)_{1-x} - (2\text{ZnSe})_x$ system.

This may be due to the excitation of vibrational modes away from the zone center. The selection rule $\vec{k}=0$ is relaxed because of the presence of substitutional disorder in the mixtures. As more ZnSe is added, the frequency of these modes gradually increases. This is to be expected since the average atomic mass of Cu and In is larger than that of Zn.

The next two modes, at 188 and 196 cm^{-1} in pure CuInSe_2 , were seen only for the compounds with the chalcopyrite structure. This agrees with our assignment of these two modes as originating from the W_2 point of the zinc-blende analog. In the zinc-blende phase, these modes are not allowed because of the $\vec{k}=0$ selection rule. In the chalcopyrite phase, the W_2 point folds into Γ_4 and becomes allowed (Table I).

The other modes in the infrared data were weak and were observed only for the pure CuInSe_2 compound but not for the mixtures. These are found at 78 and 153 cm^{-1} for pure CuInSe_2 . They must have symmetry Γ_5 as they were observed only for $\vec{E} \perp \vec{c}$.

RAMAN SCATTERING

The results of our Raman-scattering experiments are shown in Fig. 3 for pure CuInSe_2 , in Fig. 4 for $(\text{CuInSe}_2)_{0.92} - (2\text{ZnSe})_{0.08}$, and in Fig. 5 for compositions near the structural change.

Ten modes were observed for the pure CuInSe_2 crystal. To identify these modes, we use arguments from: (i) Raman selection rules for different polarizations, (ii) comparison with the infrared data, (iii) comparison with data for

TABLE II. Observed infrared-active modes of the $(\text{CuInSe}_2)_{1-x} - (2\text{ZnSe})_x$ system.

Composition	ν_{TO} (cm^{-1})	ν_{LO} (cm^{-1})	
CuInSe_2	B_2 -modes	188	196
		248	274
	E modes	78	78
		153	153
$(\text{CuInSe}_2)_{0.92} - (2\text{ZnSe})_{0.08}$		188	191
		248	274
		188	191
$(\text{CuInSe}_2)_{0.92} - (2\text{ZnSe})_{0.08}$		208	234
		183	196
$(\text{CuInSe}_2)_{0.79} - (2\text{ZnSe})_{0.21}$		201	243
		179	186
$(\text{CuInSe}_2)_{0.57} - (2\text{ZnSe})_{0.43}$		193	246
		194	248
$(\text{CuInSe}_2)_{0.52} - (2\text{ZnSe})_{0.48}$	194	248	
$(\text{CuInSe}_2)_{0.4} - (2\text{ZnSe})_{0.6}$	196	249	
ZnSe	205	253	

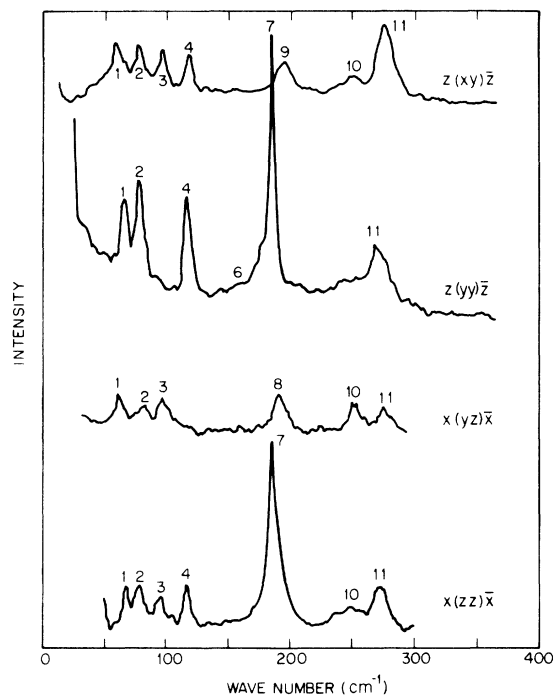


FIG. 3. Raman spectra of CuInSe_2 for different polarizations.

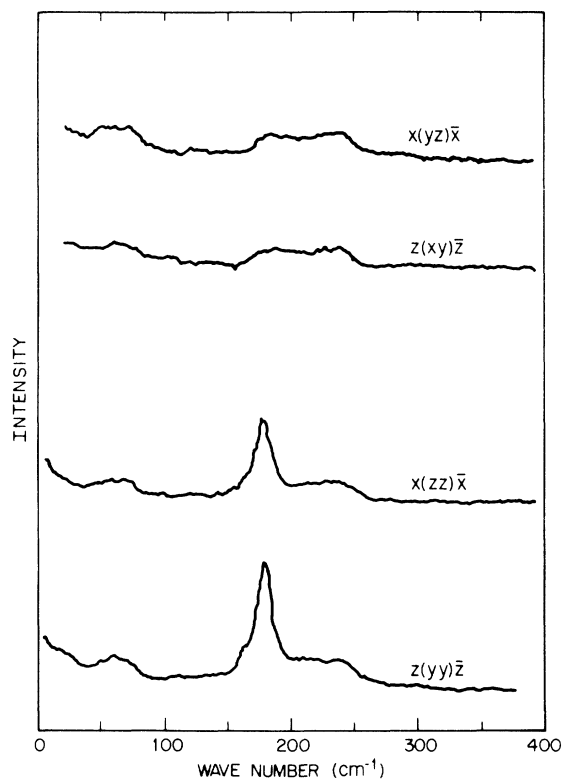


FIG. 4. Raman spectra of $(\text{CuInSe}_2)_{0.92} - (2\text{ZnSe})_{0.08}$ for different polarizations.

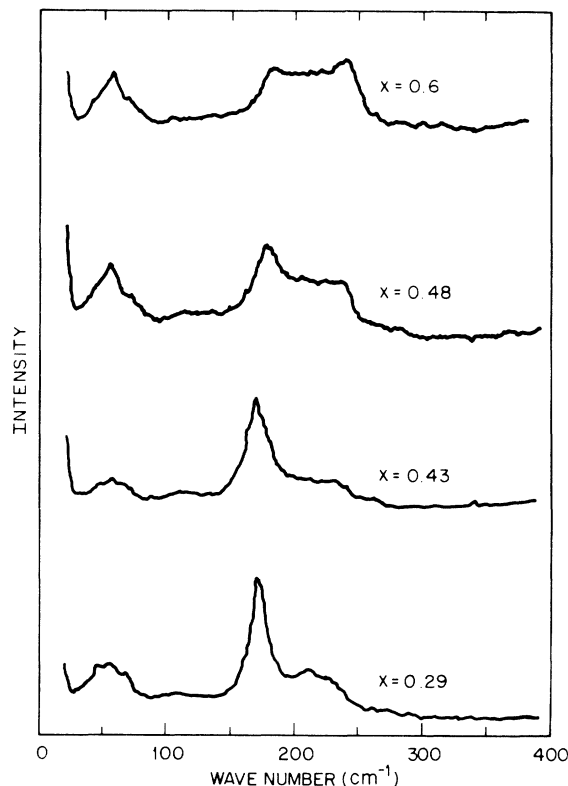


FIG. 5. Unpolarized Raman spectra of the $(\text{CuInSe}_2)_{1-x} - (2\text{ZnSe})_x$ system for different compositions.

AgGaSe_2 , (iv) comparison with data for ZnSe , and (v) comparison with data for the mixtures $(\text{CuInSe}_2)_{1-x} - (2\text{ZnSe})_x$.

The most intense mode at 186 cm^{-1} (peak 7 in Fig. 3) for pure CuInSe_2 has the symmetry assignment A_1 because it was seen only for the $z(yy)\bar{z}$ and $x(zz)\bar{x}$ polarizations. Another reason for the assignment is that the A_1 mode results from the motion of the group VI atom in the x, y plane with the group I and group III atoms at rest.¹⁴ Since the sum of the atomic masses of Cu and In are almost equal to the sum of the atomic masses of Ag and Ga (178.36 compared with 177.59 , respectively), one would expect the A_1 mode for AgGaSe_2 and CuInSe_2 to be very close. This is indeed the case, as the A_1 mode is at 179 cm^{-1} for AgGaSe_2 (as observed by van der Ziel *et al.*⁵) and at 186 cm^{-1} for CuInSe_2 . We also note that the A_1 mode is observed to be the strongest mode in AgGaSe_2 ,⁵ and in AgGaS_2 .⁸

The mode at 117 cm^{-1} (peak 4 in Fig. 3) is difficult to assign from consideration only of the polarization dependence because of depolarization effects.^{8,16} However, from comparison with the modes for AgGaSe_2 ,⁵ we assigned this mode the B_1 symmetry. The reason is as follows.

Using the results of Kaminow *et al.*,¹⁴ the low-

TABLE III. Vibrational modes of CuInSe₂ obtained from Raman and infrared spectra.

Vibrational mode (observed in Raman and ir) (cm ⁻¹)	Symmetry assignment	Experimental evidence			Origin from zinc-blende analog
		Raman	Infrared	Other	
61 (Raman)	Γ ₅ (E)	Appears in x(yz) \bar{x} [however, also in z(xy) \bar{z} , z(yy) \bar{z} , and x(zz) \bar{x}]			X ₅
78(Raman), 78 (ir)	Γ ₅ (E)	Appears in x(yz) \bar{x} [however, also in z(xy) \bar{z} , z(yy) \bar{z} , and x(zz) \bar{x}]	Appears only in $\bar{E} \perp \bar{c}$		W ₄
96 (Raman)	Γ ₄ (B ₂)	Appears in z(xy) \bar{z} [however, also in x(yz) \bar{x} and x(zz) \bar{x}]			W ₂
117 (Raman)	Γ ₃ (B ₁)	Appears in z(yy) \bar{z} [however, also in z(xy) \bar{z} and x(zz) \bar{x}]		B ₁ mode for AgGaSe ₂ is at 125 cm ⁻¹ .	W ₂
153 (ir)	Γ ₅ (E)		Appears only in $\bar{E} \perp \bar{c}$		W ₃
158 (Raman)	Γ ₃ (B ₁)	Appears only in z(yy) \bar{z}			X ₃
186 (Raman)	Γ ₁ (A ₁)	Appears only in z(yy) \bar{z} and x(zz) \bar{x}		A ₁ mode for AgGaSe ₂ is at 179 cm ⁻¹ . Since A ₁ mode depends only on the group VI atom, the A ₁ mode for AgGaSe ₂ and CuInSe ₂ should be close in energy.	W ₁
191 (Raman), 188(ir)TO 191(ir)LO	Γ ₅ (E)	Appears only in x(yz) \bar{x}	Appears only in $\bar{E} \perp \bar{c}$	Most probably originating from W ₄ because the mode disappears (in ir data) when going from x = 0.43 to 0.48.	W ₄
194(Raman), 188(ir)TO 196(ir)LO	Γ ₄ (B ₂)	Appears only in z(xy) \bar{z}	Appears only in $\bar{E} \parallel \bar{c}$		W ₂
252(Raman), 248(ir)TO	Γ ₄ + Γ ₅ (TO)	Appears in z(xy) \bar{z} and x(yz) \bar{x} [however, also in x(zz) \bar{x}]	Appears in both $\bar{E} \perp \bar{c}$ and $\bar{E} \parallel \bar{c}$	These modes were traced (in the ir data) from CuInSe ₂ to ZnSe.	Γ ₁₅ (TO)
275(Raman), 274(ir)LO	Γ ₄ + Γ ₅ (LO)	Appears in all polarizations.	Appears in both $\bar{E} \perp \bar{c}$ and $\bar{E} \parallel \bar{c}$		Γ ₁₅ (LO)

est frequency B₁ mode resembles the mode in which the group I and group III atoms move in phase and hence the mode frequency (neglecting the force constants) is proportional to (M_I + M_{III})^{-1/2}. The calculated ratio for AgGaSe₂ and CuInSe₂ from the above relation is [(107.87 + 69.72)/(63.54 + 114.82)]^{-1/2} = 1.02. The observed ratio is $\frac{145}{117} = 1.07$.

The mode at 158 cm⁻¹ has the B₁ symmetry because it was observed only in the z(yy) \bar{z} polarization. This mode is very weak because it derives from X₃, which gives very weak Raman scattering.⁸

The other modes observed, their symmetry assignments, and the possible origins from the zinc-blende analog are given in Table III.

A comparison of our assignments for CuInSe₂ and the assignments for³ ZnSe and⁵ AgGaSe₂ are shown in Fig. 6. The energy range for the vibrational modes of AgGaSe₂ and CuInSe₂ are very close because of their similar masses and positions in the periodic table.

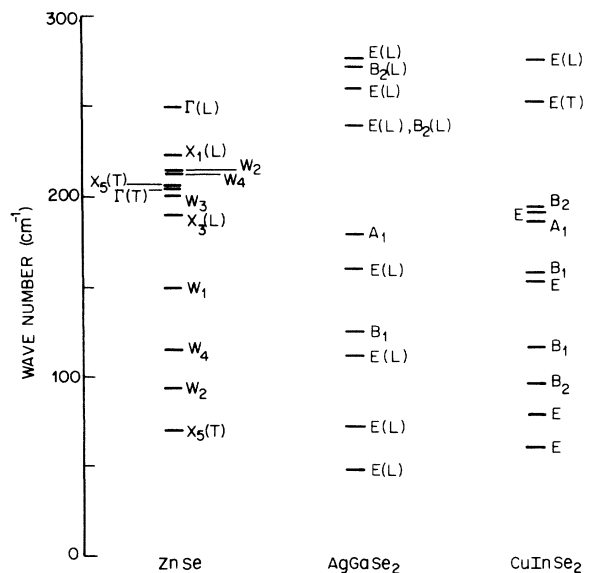


FIG. 6. Comparison of the vibrational modes of ZnSe³, AgGaSe₂⁵, and CuInSe₂.

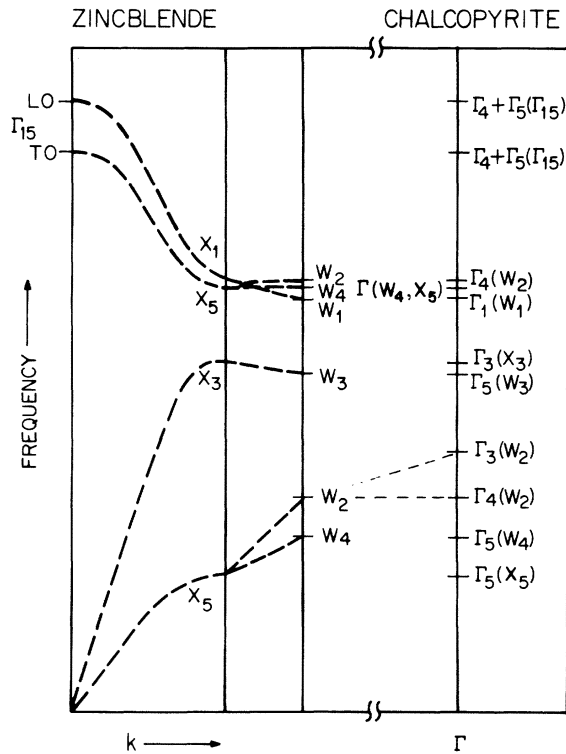


FIG. 7. Vibrational modes of CuInSe_2 at Γ and the dispersion curves of its zinc-blende analog.

If we use the relation of correspondence between the states of the zb and ch structures we can draw the phonon-dispersion relations of the ch structure in the hypothetical zb Brillouin zone (Fig. 7). In this representation, the Brillouin zone of the chalcopyrite structure is obtained by folding the hypothetical zb Brillouin zone. The dispersion relations of CuInSe_2 significantly differ from those of ZnSe . In particular, the Γ_{15} states have much higher energies than in ZnSe , and the k dependence of the frequency of the corresponding bands in the Δ direction is much more pronounced (this band is rather flat³ in ZnSe). This observation applies also to AgGaSe_2 .⁵

Raman spectra of the mixtures as shown in Figs. 4 and 5 do not show sharp structures as the

pure compound does. This can be explained again, as in the infrared spectra, by the presence of substitutional disorder in the mixtures. The Raman selection rule $\vec{k}=0$ is relaxed as a result of this disorder and modes away from the center of the Brillouin zone become allowed. The spectra, therefore, have features related to the density of the phonon states, as is the case in amorphous materials.¹⁷

The strongest peaks observed in the mixtures have the same polarization dependence as the A_1 mode in CuInSe_2 . This indicates that the \vec{k} selection rules are not completely relaxed and that the intensity of Raman scattering should be a convolution of the density of states multiplied by a \vec{k} -dependent factor. Even in amorphous semiconductors the Raman spectra contain a significant contribution from strong modes of the corresponding crystalline state.¹⁸ Since the A_1 mode involves motion of the Se atom alone, we expect its frequency to be insensitive to the composition in our mixtures as is observed.

The low-frequency bands (at about 55 cm^{-1}) and the high-frequency bands (above 200 cm^{-1}) appear to be associated with the densities of vibrational states of the TO acoustic and optic branches, respectively (cf. Fig. 7).

Another interesting feature is the similarity of the Raman spectra between the compositions $(\text{CuInSe}_2)_{0.52}-(2\text{ZnSe})_{0.48}$ and $(\text{CuInSe}_2)_{0.57}-(2\text{ZnSe})_{0.43}$. These two mixtures differ little in composition but one has a zinc-blende structure while the other has a chalcopyrite structure. This is in agreement with our suggestion that the intensity distribution in the spectra is related to the density of vibrational states since we expect that this density is not affected by zone folding.

ACKNOWLEDGMENTS

We would like to thank E. Finkman for his help and suggestions during the early stages of this work, J. H. Wernick for his interest and encouragement, and S. R. Nagel for his helpful comments on the manuscript. We also appreciate the technical assistance of T. R. Kirst.

*Work at Brown University was supported in part by a grant from AROD (DA-ARO-D-31-124-72-G204) and also by the NSF through the general support of Materials Science at Brown University.

†Also at Bell Laboratories, Murray Hill, N. J. 07974.

¹V. G. Lambrecht, Jr., Mater. Res. Bull. **8**, 1383 (1973).

²J. L. Shay and J. H. Wernick, *Ternary Chalcopyrite Semiconductors* (Pergamon, New York, 1975).

³J. C. Irwin and J. LaCombe, Can. J. Phys. **50**, 2596 (1972).

⁴J. Baars and W. H. Koschel, Solid State Commun. **11**,

1513 (1972).

⁵J. P. van der Ziel, A. E. Meixner, H. M. Kasper, and J. A. Ditzenberger, Phys. Rev. B **9**, 4286 (1974).

⁶G. D. Holah, Opt. Commun. **5**, 10 (1972).

⁷G. D. Holah and J. S. Webb, *Proceedings of the Eleventh International Conference on the Physics of Semiconductors* (Polish Scientific Publishers, Warsaw, 1972), p. 1161.

⁸G. D. Holah, J. S. Webb, and H. Montgomery, J. Phys. C **7**, 3875 (1974).

⁹W. H. Koschel, V. Hohler, A. Rauber, and J. Baars,

- Solid State Commun. 13, 1011 (1973).
- ¹⁰R. H. Parmenter, Phys. Rev. 100, 573 (1955).
- ¹¹Von R. Sandrock and J. Treusch, Z. Naturforsch. A 19, 844 (1964).
- ¹²J. N. Gan, Ph.D. thesis (Brown University, 1975) (unpublished).
- ¹³G. F. Koster, J. O. Dimmock, R. C. Wheeler, and H. Statz, *Properties of the Thirty-Two Point Groups* (M.I.T. Press, Cambridge, Mass., 1963).
- ¹⁴I. P. Kaminow, E. Buehler, and J. H. Wernick, Phys. Rev. B 2, 960 (1970).
- ¹⁵A. Arguello, D. L. Rousseau, and S. P. S. Porto, Phys. Rev. 181, 1351 (1969).
- ¹⁶M. Bettini, W. Bauhofer, M. Cardona, and R. Nitsche, Phys. Status Solidi B 63, 641 (1974).
- ¹⁷J. Tauc in *Amorphous and Liquid Semiconductors*, edited by J. Tauc (Plenum, London, 1974), p. 159.
- ¹⁸S. S. Mitra, D. K. Paul, Y. F. Tsay, and B. Bendow in *Tetrahedrally Bonded Amorphous Semiconductors*, edited by M. H. Brodski, S. Kirkpatrick, and D. Weaire (AIP, New York, 1974), p. 284.